ACS MEASUREMENT SCIENCE Au
AN OPEN ACCESS JOURNAL OF THE AMERICAN CHEMICAL SOCIETY

pubs.acs.org/measureau
Article

Single-Frequency Effective Capacitance C_{ec} and Membrane Resistance Z Readout for Solid-Contact Ion-Selective Electrodes

Tingting Han,* Sini Chen, Tao Song, Dongxue Han, and Li Niu

Cite This: ACS Meas. Sci. Au 2025, 5, 216−225
Read Online

ABSTRACT: Here, we propose new single-frequency effective capacitance C_{ec} and membrane resistance Z readout principle for solid-contact ion-selective electrodes (SCISEs). Conducting polymer poly(3,4-ethylenedioxythiophene) (PEDOT) doped with polystyrenesulfonate (PSS^-), *i.e.*, PEDOT(PSS), as solid contact and valinomycin-based membrane were prepared for K^+-SCISEs. At high frequencies, the membrane resistance of K^+-SCISEs corresponding to impedance absolute value Z was recorded constantly as KCl aqueous solution diluted with water. The membrane resistance Z increases as the electrolyte concentration decreases. Under identical dilution steps, the linear slope of the logarithmic membrane resistance log$Z$ *vs* loga_{K+} for K^+-SCISEs with the spin-coated membrane is larger than that of the electrode covered with the drop-cast membrane. As the K^+-SCISE resistance with the spin-coated membrane was reduced to hundreds of Ω, the log$Z$ of K^+-SCISEs is linearly proportional to loga_{K+} in the range of −1 to −3.4, providing a possibility of utilizing membrane resistance Z as a calibration-free analytical signal for SCISEs. The effective capacitance C_{ec} of K^+-SCISEs with the spin-coated membrane was performed in 0.1 M KCl applied with single frequency ranging from 1 MHz and decreases by a factor of 10 to 10 mHz. The obtained C_{ec} of K^+-SCISEs with the spin-coated membrane is linearly proportional to log$f$ in the range of 1 MHz to 10 Hz with a slope of *ca.* −0.97, while at a low frequency ranging from 1 Hz to 10 mHz, the linear slope of logC_{ec} *vs* log$f$ is suppressed, where Warburg diffusion takes effect. Furthermore, the membrane resistance Z is independent of applied high frequencies, and the effective capacitance C_{ec} is independent of the excitation amplitude.

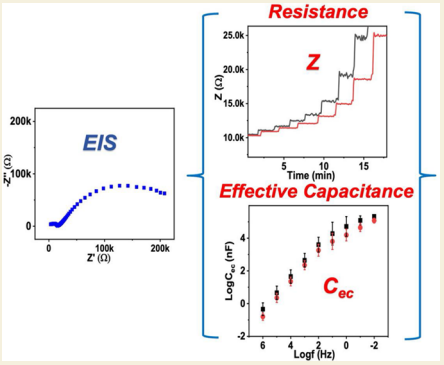

KEYWORDS: *single-frequency capacitance, membrane resistance, electrochemical impedance spectroscopy, PEDOT, solid-contact ion-selective electrodes*

1. INTRODUCTION

Ion-selective electrodes (ISEs) are cost-effective analytical sensors that are used in various applications and play a vital role in maintaining routine life.[1−6] The development of solid-contact ion-selective electrodes (SCISEs) was started by eliminating the inner filling solution to a coated-wire electrode (CWE).[7]The continuation potential stability improvement for SCISE was achieved by introducing a large-capacitance solid contact, *i.e.*, conducting polymers, carbon nanotubes, redox buffers, intercalation compound, and double-layer capacitance, to increase ion-to-electron transfer capacitance, resulting in potential stability improvement for SCISEs.[8−14]

The development of electrochemical techniques, listed as follows, but not limited to chronoamperometry,[15−19] electrochemical impedance spectroscopy (EIS),[20−23] coulometric readout,[24−27] and cyclic voltammetry[28,29] was performed for SCISEs ion detection and characterization. Chronoamperometry was used for potential stability checking of SCISEs.[16] Coulometric readout has a unique advantage of improving the sensitivity by increasing the thickness of the solid contact in comparison with potentiometry.[30] Utilizing a novel two-electrode setup in series with a capacitor was introduced, resulting in sensitivity improvement for coulometric readout.[31]

Electrochemical impedance spectroscopy (EIS) has been widely used as a powerful technique for characterization SCISEs, including the electroactive polymer property studies, the charge transfer kinetics at the ISM solution interface and also the charge transfer/ion diffusion through membrane and the capacitance of the solid contact.[20,32−39] The resistor-capacitor (RC) model of EIS for SCISE characterization is that the impedance real part Z' of EIS represents the membrane resistance and the imaginary value Z'' at 10 mHz provides the low-frequency capacitance for SCISEs, where the membrane acts as the resistor and the solid contact as the capacitor.[16,17]

The performance of the membrane resistance corresponding to the impedance real part Z' of ion-selective electrodes and

Received: December 8, 2024
Revised: March 3, 2025
Accepted: March 6, 2025
Published: March 13, 2025

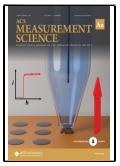

Table 1. K^+-SCISEs Experimental Preparation Parameters[a]

K^+-SCISEs	Thickness of PEDOT solid contact (mC)			Drop-cast membrane (μl)	Spin-coated membrane[&] (μl)
	1	5	10		
Polymerization time[*]	70s	350s	700s		
Cocktail volume[#]				50 (1 drop)	15 (2 drops)
1mC/drop-cast membrane					
1mC/spin-coated membrane					
5mC/drop-cast membrane					
5mC/spin-coated membrane					
10mC/drop-cast membrane					
10mC/spin-coated membrane					
Coated-wire/drop-cast membrane					
Coated-wire/spin-coated membrane					

[a]*Polymerization solution 0.01 M EDOT + 0.1 M NaPSS; [#]K^+-ISM cocktail composition: 1 wt % valinomycin, 0.5 wt % KTFPB, 1 wt % ETH-500, 65.3 wt % DOS, and 32.2 wt % PVC dissolved in THF (dry mass = 15 wt %);[&]Rotator speed at 1500 rpm for 60 s.

the internal filling solution utilizing traditional EIS was explored.[40−45] It revealed that the membrane resistance increases as the concentration of primary ions decreases. The water absorption and concentration of the interfering ions have an impact on the membrane resistance.

The EIS low-frequency capacitance corresponding to the imaginary value Z'' of EIS at 10 mHz was used for the capacitance of SCISE calculation.[22,23,38] The concentration of electrolyte solution is usually 0.1 M.[12] The large-capacitance properties of carbon nanotubes characterized by EIS low-frequency prove that carbon nanotubes can be used as ion-to-electron transducers for SCISEs.[12] Furthermore, the amount of EIS low-frequency capacitance of decorated functional materials is in close correlation with the cumulated charge of coulometric response of SCISEs.[46] The EIS low-frequency capacitance changes after Ag deposition/de-deposition on the Nafion film are also in good agreement with stripping voltammetry.[47]

In this work, instead of using the impedance real part Z' of electrochemical impedance spectrum representing membrane resistance at semicircle high frequency, a new membrane resistance corresponding to the impedance absolute value Z of K^+-SCISEs was recorded with time as KCl aqueous solution diluted with water at $\Delta \log a_{K+}$ = 0.3 decades/step. The membrane resistance Z performance of K^+-SCISEs with CWEs, 1, 5, and 10 mC poly(3,4-ethylenedioxythiophene) doped with polystyrenesulfonate (PEDOT(PSS)) solid contact covered with drop-cast or spin-coated membrane was studied in detail and applied with semicircle high frequency. The obtained membrane resistance of K^+-SCISEs is dependent on the concentration of KCl and also the thickness of the membrane. The effective capacitance C_{ec} of K^+-SCISEs covered with the spin-coated membrane performed in 0.1 M KCl applied with single frequency ranging from 1 MHz and decreases by a factor of 10 to 10 mHz. The resulting effective capacitance of K^+-SCISEs increases as the applied frequency decreases. The linear correlation of the logarithmic effective capacitance $\log C_{ec}$ of PEDOT-based K^+-SCISEs with respect to $\log f$ was also studied. In comparison with the applied frequency, the excitation amplitude impact on the effective capacitance of PEDOT-based K^+-SCISEs is almost negligible.

2. EXPERIMENTAL PART

2.1. Reagents and Materials

Valinomycin, potassium tetrakis[3,5-bis(trifluoromethyl)-phenyl]-borate (KTFPB), bis(2-ethylhexyl)sebacate (DOS), poly(vinyl chloride) (PVC), tetradodecylammonium tetrakis(4-chlorophenyl)-borate (ETH-500), 3,4-ethylenedioxythiophene (EDOT, 97%), poly(sodium 4-styrenesulfonate) (NaPSS, $M_W \approx$ 70,000), and tetrahydrofuran (THF) were purchased from Sigma-Aldrich and were of Selectophore purity grade. Potassium chloride (KCl, ≥99.5%) and sodium chloride (NaCl, ≥99%) were purchased from Sigma-Aldrich. Deionized water (resistivity > 18.2 MΩcm) was used for all experiments, which was produced using an ultrapure water system from Sichuan Waterpure Instrument Co. Ltd, China.

2.2. Electrode Preparation

Glassy carbon (GC) disk electrodes (Φ = 3 mm) with PVC bodies were first polished with diamond paste of 1 and 0.3 μm Al_2O_3 powder. Then, the well-polished electrodes were ultrasonicated in ethanol and water baths for 5 min separately. Polymerization solution containing 0.01 M EDOT and 0.1 M NaPSS was prepared by stirring constantly for at least 5 h for a complete monomer dissolution at room temperature. The polymerization solution was purged with N_2 gas for *ca.* 15 min, and the gas flow was kept above the solution to avoid oxygen during polymerization.

Conducting polymers PEDOT(PSS) was electrochemically deposited on the surface of GC using chronopotentiometry with a CHI 1030C electrochemical workstation (Shanghai Chenhua Apparatus). A constant current of 0.014 mA (current density = 0.2 mA/cm^2) was applied for 70, 350, and 700 s to produce the corresponding 1, 5, and 10 mC PEDOT(PSS) polymerization charge, respectively. After polymerization, the GC/PEDOT(PSS) electrodes were rinsed with deionized water and kept dry in ambient air overnight.

The K^+-ISM was drop-cast in one 50 μL aliquot of the K^+-ISM cocktail (dry mass = 15 wt %) covering the whole surface area of bare GC electrode and the GC electrode with 1 and 5 mC PEDOT(PSS) solid contact, including the PVC body of each electrode. Spin-coated thin-layer membrane was prepared by dropping 15 μL of cocktail two times (30 μL in total) on the electrode surface by holding the rotator with a rotating speed of 1500 rpm for 60 s. A thin layer of membrane was uniformly dispersed on the electrode surface, while the excess of cocktail was spinning out. The composition of the K^+-ISM was 1 wt % valinomycin, 0.5 wt % KTFPB, 1 wt % ETH-500, 65.3 wt % DOS, and 32.2 wt % PVC dissolved in THF (dry mass = 15 wt %). The membranes were left to dry at room temperature for at least 4 h, followed by overnight conditioning of the K^+-SCISEs in 0.1 M KCl before the measurements, and stored in 0.1 M KCl between the

https://doi.org/10.1021/acsmeasuresciau.4c00093
ACS Meas. Sci. Au 2025, 5, 216−225

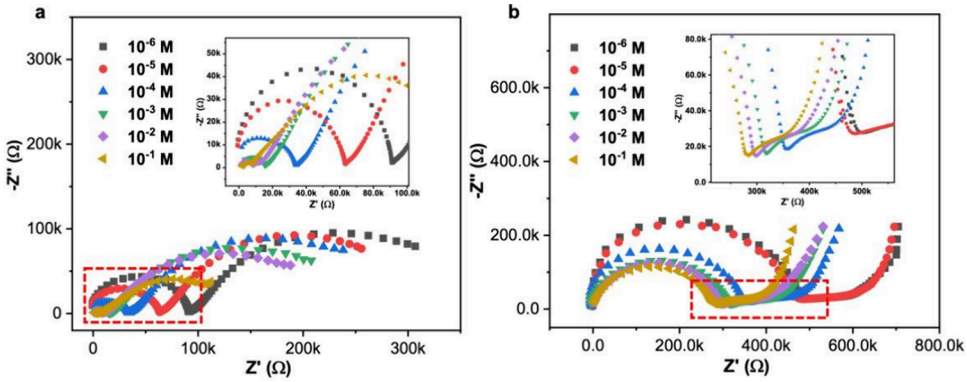

Figure 1. Electrochemical impedance spectrum of K^+-SCISEs with 1 mC PEDOT(PSS) covered with spin-coated membrane (a) and 5 mC PEDOT(PSS) with drop-cast membrane (b) measured in KCl solution concentration ranging from 10^{-1} to 10^{-6} M KCl. The insets of Figure 1a,b are partial enlargements of each EIS spectrum.

experiments. The K^+-SCISEs experimental preparation parameters are shown in Table 1.

2.3. Potentiometric Calibration of K^+-SCISEs

The performance of the well-prepared K^+-SCISEs with coated-wire, 1, 5, and 10 mC PEDOT(PSS) solid contact covered with spin-coated and drop-cast membranes was checked by potentiometric calibration utilizing instrument EMF 16 (Lawson Lab, Inc.) before EIS. K^+-SCISE was used as the working electrode, and a double junction Ag/AgCl/3 M KCl/1 M LiAc was used as the reference electrode. The calibration slope of K^+-SCISEs was *ca.* 55 ± 2 mV/decades, ranging from 10^{-1} to 10^{-6} M KCl aqueous solution, corresponding to Nernst equation. With the presence of the constant ionic background 0.1 M NaCl, the Nernst slope of K^+-SCISEs maintains[2−4] (Supporting Information).

2.4. EIS of K^+-SCISEs

Traditional EIS for K^+-SCISEs with 1 mC PEDOT(PSS) covered with the spin-coated membrane and 5 mC PEDOT(PSS) covered with the drop-cast membrane was performed in KCl aqueous solution with concentration ranging from 10^{-1} to 10^{-6} M at open-circuit potential (OCP) using the Gamry reference 600 plus electrochemical workstation in a three-electrode electrochemical cell. A single junction Ag/AgCl/3 M KCl was used as the reference electrode, and a platinum rod was used as the counter electrode. The EIS wide-frequency conversion process was ranging from 1 MHz to 10 mHz. The excitation amplitude was 10 mV (RMS).

2.5. Membrane Resistance *Z* of PEDOT-Based K^+-SCISEs with Semicircle High Frequency

EIS of K^+-SCISEs membrane resistance applied with semicircle high frequency was performed utilizing a CHI760 electrochemical workstation (Shanghai Chenhua Apparatus). K^+-SCISEs with coated-wire, 1, 5, and 10 mC PEDOT(PSS) covered with spin-coated or drop-cast membrane were performed as the working electrode, Pt as the counter electrode, and a single junction Ag/AgCl/3 M KCl as the reference electrode. The membrane resistance *Z* of K^+-SCISEs was recorded with starting solution as 10 mL of 0.1 M KCl diluted with 5 mL of deionized water or 10 mL of 0.1 M KCl + 0.1 M NaCl diluted with 5 mL of 0.1 M NaCl as a constant ionic background with $\Delta \log a_{K+} = 0.3$ decades/step. The EIS semicircle high frequency was set as the applied frequency for the K^+-SCISEs membrane resistance *Z* measurement (Figures 2−4).

The EIS membrane resistance *Z* of K^+-SCISEs with 5 mC PEDOT(PSS) solid contact covered with spin-coated membrane was performed with high frequencies ranging from 1 MHz to 0.1 kHz, *i.e.*,1 MHz, 0.1 MHz, 10 kHz, 1 kHz, and 0.1 kHz (Figure 5). The aqueous solution of 10 mL 0.1 M KCl was diluted with 5 mL of water at $\Delta \log a_{K+} = 0.3$ decades/step. The concentration of primary ion K^+ was from 10^{-1} to 10^{-5} M.

2.6. Single-Frequency Effective Capacitance C_{ec} of PEDOT-Based K^+-SCISEs Ranging from 1 MHz Decreases by a Factor of 10 to 10 mHz

The EIS single-frequency effective capacitance C_{ec} of K^+-SCISEs with coated-wire, 1, 5, and 10 mC PEDOT(PSS) covered with the spin-coated membrane was performed with Gamry reference 600 plus electrochemical workstations. The applied EIS single frequency was ranged from 1 MHz decreases by a factor of 10 to 10 mHz, *i.e.*, 1 MHz, 0.1 MHz, 10 kHz, 1 kHz, 0.1 kHz, 10 Hz, 1 Hz. 0.1 Hz, and 10 mHz. Time scale is 0.1 h (6 min). The excitation amplitude was fixed at 10 mV (RMS). The applied potential was setting at 0 V with respect to open-circuit potential (OCP). A single junction Ag/AgCl/3 M KCl was used as the reference electrode, and Pt was used as the counter electrode. K^+-SCISEs with coated-wire, 1, 5, and 10 mC PEDOT(PSS) solid contact covered with spin-coated membrane were performed as the working electrodes.

The EIS excitation amplitude impact on the effective capacitance C_{ec} of SCISEs in combination with applied single frequency was performed for K^+-SCISEs with 5 mC PEDOT(PSS) solid contact covered with spin-coated membrane. The excitation amplitude was set at 5, 10, 20, 30, and 50 mV. The applied EIS frequency parameters range from 1 MHz and decrease by a factor of 10 to 10 mHz, i.e., 1 MHz, 0.1 MHz, 10 kHz, 1 kHz, 0.1 kHz, 10 Hz, 1 Hz, 0.1 Hz, and 10 mHz.

3. RESULTS AND DISCUSSION

3.1. Traditional EIS of PEDOT-Based K^+-SCISEs

Traditional electrochemical impedance spectrum of K^+-SCISEs with 1 mC PEDOT(PSS) covered with the spin-coated membrane and 5 mC PEDOT(PSS) covered with the drop-cast membrane with frequency conversion from 1 MHz to 10 mHz was measured in KCl aqueous solution with concentration ranging from 10^{-1} to 10^{-6} M (Figure 1). As the semicircle high frequency of EIS represents K^+-selective bulk membrane resistance, it is clear that the K^+-selective spin-coated bulk membrane resistance is in the range of 10 to 100 KΩ at KCl concentration ranging from 10^{-1} to 10^{-6} M (Figure 1a), while for the drop-cast membrane, it is from 240 to 500 KΩ (Figure 1b). The K^+-selective bulk membrane resistance roughly follows the trend, the EIS semicircle bulk membrane resistance increases as the concentration of KCl aqueous solution decreases.[41−43]

As described above, the impedance imaginary value *Z″* of the electrochemical impedance spectrum at 10 mHz for K^+-SCISEs can be used for solid contact capacitance estimation. The EIS low-frequency capacitance of K^+-SCISEs with 1 mC PEDOT(PSS) covered with the spin-coated membrane

https://doi.org/10.1021/acsmeasuresciau.4c00093
ACS Meas. Sci. Au 2025, 5, 216−225

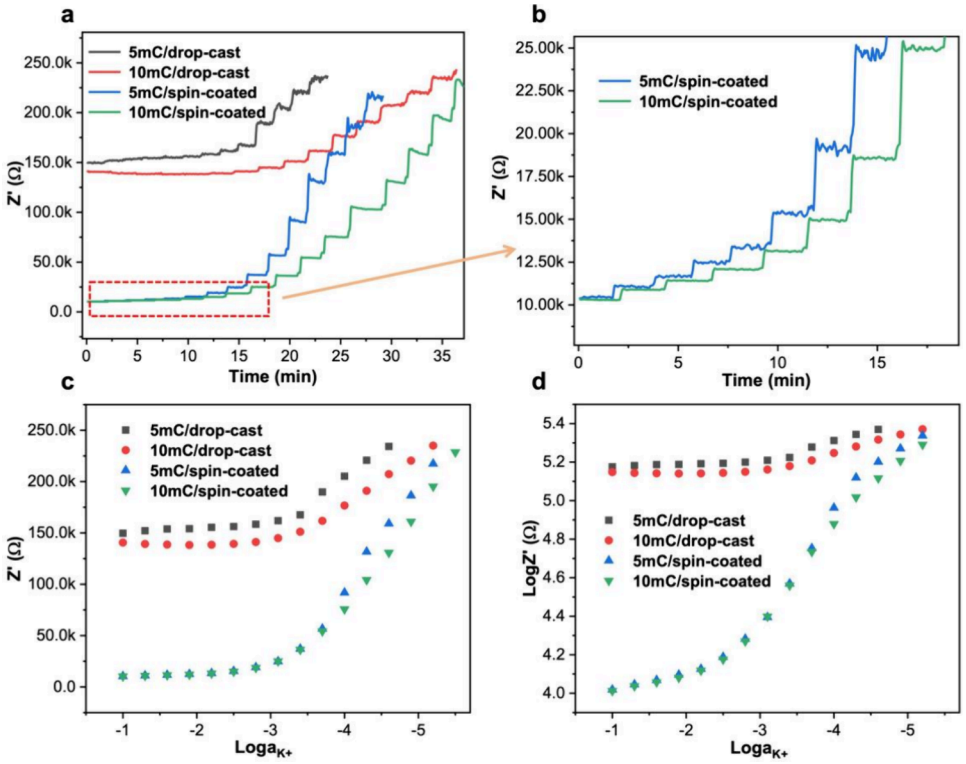

Figure 2. (a) The membrane resistance Z of K^+-SCISEs with 5 and 10 mC PEDOT(PSS) as solid contact covered with drop-cast and spin-coated membranes *vs* time. The dilution was started with 0.1 M KCl diluted with deionized water with $\Delta\log a_{K+}$ = 0.3 decades/step. (b) Enlarged section of membrane resistance Z *vs* time. (c) Membrane resistance Z *vs* $\log a_{K+}$. (d) log$Z$ *vs* $\log a_{K+}$. The corresponding semicircle high frequency for each electrode is 5 mC/drop-cast (1600 Hz), 10 mC/drop-cast (1000 Hz), 5 mC/spin-coated (1650 Hz), and 10 mC/spin-coated (15,890 Hz).

(Figure 1a) at 10 mHz is even larger than the corresponding K^+-SCISEs with 5 mC PEDOT(PSS) solid contact and drop-cast membrane (Figure 1b), indicating ion transfer was limited by the large impedance of the thick drop-cast membrane. The low-frequency capacitance of 5 mC PEDOT(PSS) solid contact is suppressed. The obtained low-frequency capacitance of K^+-SCISEs with 5 mC PEDOT with drop-cast membrane at 10 mHz shows rather an equivalent amount with the KCl concentration ranging from 10^{-1} to 10^{-6} M (Figure 1b).[48]

3.2. Membrane Resistance *Z* of PEDOT-Based K^+-SCISEs with Semicircle High Frequency

Instead of utilizing the impedance real part Z' of traditional electrochemical impedance spectrum at semicircle high frequency for membrane resistance (Figure 1), a new membrane resistance of K^+-SCISEs corresponding to the impedance absolute value Z was constantly recorded with the KCl aqueous solution diluted with water. As shown in Figure 2a,b, the staircase membrane resistance Z of K^+-SCISEs with 5 and 10 mC PEDOT(PSS) as the solid contact covered with drop-cast and spin-coated membranes increases as the concentration of KCl aqueous solution gradually decreases at $\Delta\log a_{K+}$ = 0.3 decades/step. The enlargement of membrane resistance Z for K^+-SCISEs with a spin-coated membrane (*ca.* 10 KΩ) started increasing with KCl dilution at the beginning concentration of 10^{-1} M (Figure 2b) but not for the K^+-SCISEs with a drop-cast membrane (*ca.* 150 KΩ) due to its large impedance of the thick membrane.

As shown in Figure 2c, when K^+-SCISEs are covered with the drop-cast membrane (*ca.* 150 KΩ), the membrane resistance increasing starts at $\log a_{K+}$ *ca.* -3.5, while for the spin-coated membrane (*ca.* 10 KΩ), it starts at $\log a_{K+}$ −3.[41]

The increasing membrane resistance Z (*ca.* 10 KΩ) of K^+-SCISEs with the spin-coated membrane is larger than that of the drop-cast membrane (*ca.* 150 KΩ), while the logarithmic K^+ activity is ranging from −3.5 to −5 (Figure 2c). Similarly, it is also obvious to see that the linear slope of the logarithmic membrane resistance log$Z$ of K^+-SCISEs with the spin-coated membrane *vs* $\log a_{K+}$ in the range of −3 to −5 is larger than that of the electrode with the drop-cast membrane (Figure 2d).

In brief, log$Z$ increases as $\log a_{K+}$ decreases. Under identical dilution steps, the linear slope of log$Z$ *vs* $\log a_{K+}$ for K^+-SCISEs with the spin-coated membrane is larger than that for the electrodes covered with the drop-cast membrane. As the logarithmic activity of primary ion K^+ was diluted from −1 to −5, the membrane resistance Z of K^+-SCISEs is dependent on the concentration of KCl and also the thickness of the membrane.

The membrane resistance Z of K^+-SCISEs with coated-wire and 1 mC PEDOT(PSS) covered with spin-coated membrane was recorded constantly with time as starting solution 0.1 M KCl diluted with water at $\Delta\log a_{K+}$ = 0.3 decades/step with semicircle high frequency for each electrode (Figure 3a). The membrane resistance Z increases as the KCl concentration decreases. What is more interesting is that as the membrane resistance of K^+-SCISEs with a spin-coated membrane was reduced to *ca* hundreds Ω in 0.1 M KCl (Figure 3c), the obtained logarithmic membrane resistance log$Z$ gives a linear response to $\log a_{K+}$ ranging from −1 to −3.4 (Figure 3c). As the K^+-SCISEs with 1 mC PEDOT(PSS) covered with spin-coated membrane resistance increases from hundreds Ω to 10 KΩ, the linear slope of log$Z$ *vs* $\log a_{K+}$ decreases.

https://doi.org/10.1021/acsmeasuresciau.4c00093
ACS Meas. Sci. Au 2025, 5, 216−225

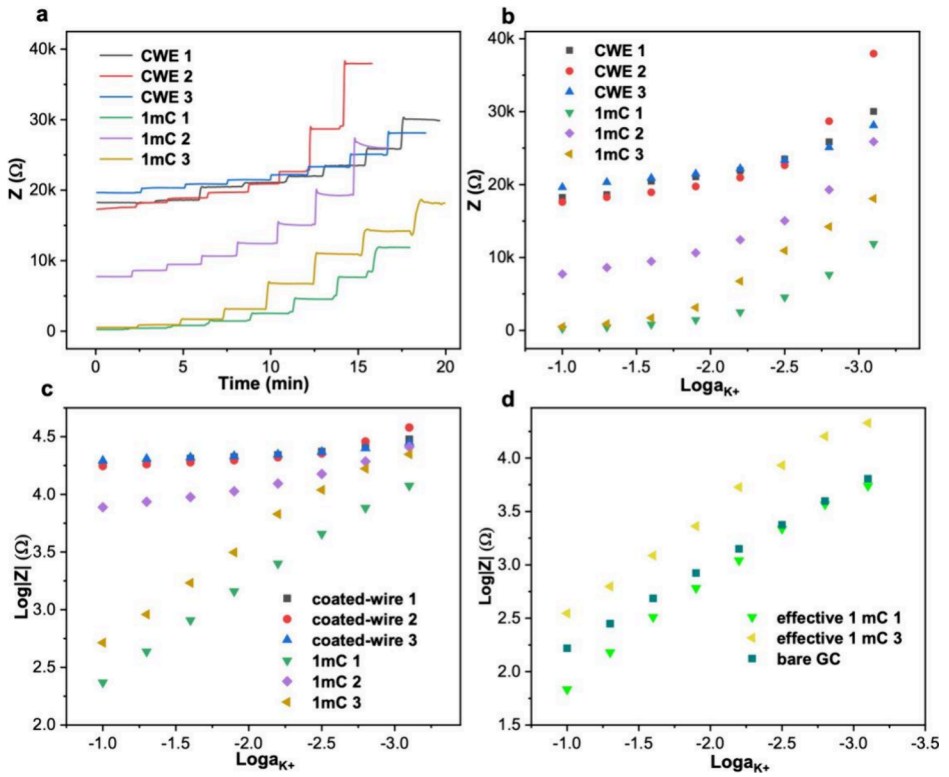

Figure 3. (a) The membrane resistance Z of K^+-SCISEs with coated-wire and 1 mC PEDOT(PSS) solid contact covered with spin-coated membrane applied with semicircle high frequency *vs* time. The dilution was started with 0.1 M KCl aqueous solution diluted with deionized water at $\Delta\log a_{K+} = 0.3$ decades/step. (b) Membrane resistance Z *vs* $\log a_{K+}$. (c) $\log Z$ *vs* $\log a_{K+}$. (d) The logarithmic resistance of bare GC and membrane resistance $\log Z$ of K^+-SCISEs *vs* $\log a_{K+}$. The corresponding semicircle high frequency for each electrode is CWE 1 (1976 Hz), CWE 2 (252 Hz), CWE 3 (158 Hz), 1 mC 1 (25170 Hz), 1 mC 2 (198 Hz), 1 mC 3 (31640 Hz), and bare GC (1000 Hz).

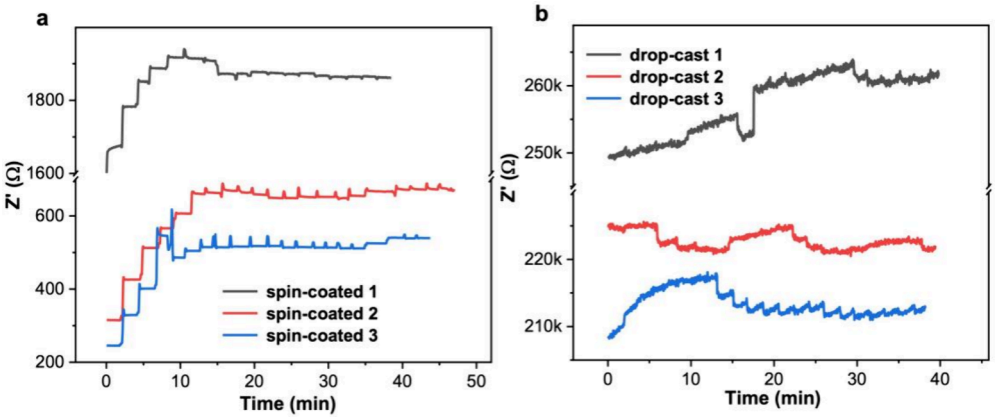

Figure 4. EIS membrane resistance Z of K^+-SCISEs with 5 mC PEDOT(PSS) as solid contact covered with spin-coated (a) and drop-cast (b) membranes applied with semicircle high frequency vs time, with the KCl concentration ranging from 10^{-1} M diluted to 10^{-7} M with $\Delta\log a_{K+} = 0.3$ decades/step. The corresponding semicircle high frequency is spin-coated 1 (12,910 Hz), spin-coated 2 (20,020 Hz), spin-coated 3 (10,080 Hz), drop-cast 1 (796 Hz), drop-cast 2 (627 Hz), and drop-cast 3 (317 Hz).

Excluding the resistance of bare GC to KCl aqueous solution diluted with water at $\Delta\log a_{K+} = 0.3$ decades/step, the resulting logarithmic effective resistance $\log Z$ of K^+-SCISEs with 1 mC PEDOT and spin-coated membrane still gives a linear response with respect to $\log a_{K+}$ in the range of -1 to -3.3, while the membrane resistance of spin-coated membrane plus PEDOT is *ca.* hundreds Ω in 0.1 M KCl (Figure 3d), providing a possibility of utilizing membrane resistance Z as a calibration-free analytical signal for SCISEs in pure KCl aqueous solution.

The membrane resistance Z of PEDOT-based K^+-SCISEs with 5 mC PEDOT(PSS) covered with spin-coated and drop-cast membrane was recorded for *ca.* 40 min with the starting solution of 0.1 M KCl + 0.1 M NaCl diluted with 0.1 M NaCl as the constant ionic background at $\Delta\log a_{K+} = 0.3$ decades/step for 20 steps (Figure 4a,b). As the membrane resistance of K^+-SCISEs with spin-coated membrane increases ranging from hundreds Ω to KΩ (Figure 4a), the membrane resistance Z starts increasing at the beginning 5−7 dilution steps, due to the KCl concentration decreasing at $\Delta\log a_{K+} = 0.3$ decades/step, and then the membrane resistance Z maintains a stable impedance, where the impedance is dependent on the K^+-SCISE membrane response to 0.1 M NaCl. As shown in Figure

https://doi.org/10.1021/acsmeasuresciau.4c00093
ACS Meas. Sci. Au 2025, 5, 216−225

4b, with the presence of a strong electrolyte 0.1 M NaCl, the impedance of the K^+-SCISEs with 5 mC PEDOT(PSS) and drop-cast membrane shifts in the range of 210 to 260 KΩ, attributed to the large impedance of the thick membrane, while the KCl aqueous solution concentration ranges from 10^{-1} to 10^{-7} M.

The membrane resistance Z of PEDOT-based K^+-SCISEs with 5 mC PEDOT(PSS) covered with spin-coated membrane was performed with multiple high frequencies, *i.e.*, 1 MHz. 0.1 MHz, 10 kHz, 1 kHz, and 0.1 kHz (Figure 5a). The membrane resistance increases as the concentration of KCl aqueous solution decreases, as described above (Figure 3a). The obtained results of logarithmic membrane resistance log$Z$ behave independent of the applied high frequencies (Figure 5b), indicating that high frequencies have a minor impact on the membrane resistance Z. This is also in good agreement with EIS model circuits in the case of high frequencies where φ = 0°, where the EIS response is dominated by the resistance and thus is independent of the frequency.[49] The logarithmic membrane resistance log$Z$ gives a rather linear response with respect to loga_{K+} in the range −1 to −4 (Figure 5c).

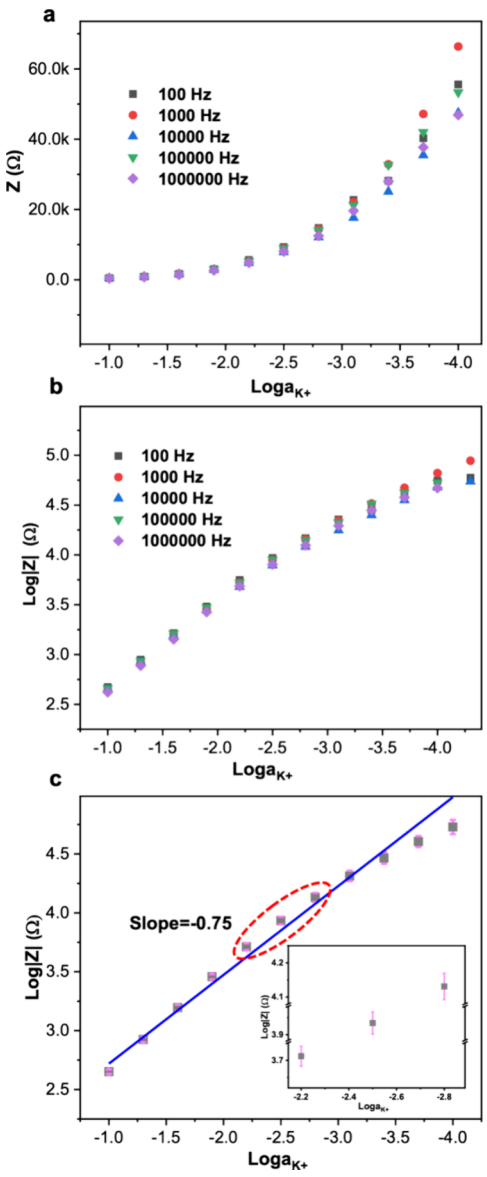

Figure 5. (a) The membrane resistance Z of the PEDOT-based K^+-SCISE with 5 mC PEDOT(PSS) as solid contact covered with spin-coated membrane performed with multiple high frequencies, *i.e.*,1 MHz, 0.1 MHz, 10 kHz, 1 kHz, and 0.1 kHz, with loga_{K+} ranging from −1 to −4. (b) log$Z$ *vs* loga_{K+}. (c) The corresponding log$Z$ of the K^+-SCISE (Figure 5a) with variable applied high frequencies *vs* loga_{K+} with error bar, inset is the partial enlargement.

3.3. Single-Frequency Effective Capacitance C_{ec} of PEDOT-Based K^+-SCISEs Ranging from 1 MHz and Decreases by a Factor of 10 to 10 mHz

The K^+ ion transfer mechanism of PEDOT-based K^+-SCISEs and the corresponding equivalent circuit was shown in Figure 6a.[17] Conducting polymer PEDOT(PSS) was performed as ion-to-electron transducer based on its $PEDOT^+/PEDOT^0$, doping/undoping ability with target ions.[16] The capacitance of PEDOT play a vital role for the amount of ion transfer through PEDOT solid contact, acting as capacitor (C_{PEDOT}) and K^+-selective valinomycin membrane as resistor (R_b) (Figure 6a).[17]

The traditional electrochemical impedance spectrum of K^+-SCISEs with 10 mC PEDOT(PSS) and spin-coated membrane performed in 0.1 M KCl with frequency conversion from 1 MHz to 10 mHz is shown in Figure 6b,c, where the impedance real part Z' at the semicircle high frequency point represents the membrane resistance (*ca.* 320 Ω) and the low-frequency imaginary value Z'' at 10 mHz can be used for PEDOT solid contact capacitance calculation (*ca.* 265 μF) according to the calculation equation $C = -1/(2\pi f Z'')$. As shown in Figure 6d,e, the effective capacitance C_{ec} of K^+-SCISEs with 5 mC PEDOT(PSS) solid contact and spin-coated membrane performed in 0.1 M KCl applied with single frequency for 6 min ranging from 1 MHz decreases by a factor of 10 to 10 mHz. Each applied frequency results in a rather stable, almost constant capacitance over 6 min. The effective capacitance decreases as the applied frequency increases. The effective capacitance C_{ec} of K^+-SCISEs is the recording data with time when frequency in combination with excitation amplitude was applied corresponding to the impedance absolute value Z. The calculation equation is $C_{ec} = 1/(2\pi f Z)$, where f is the applied frequency and Z is the impedance absolute value.

As shown in Figure 6f, at low frequencies ranging from 1 Hz to 10 mHz, the resulting effective capacitance increases as the thickness of solid contact increases in sequence from CWEs, 1, 5, to 10 mC PEDOT(PSS), indicating that more portion of $PEDOT^+/PEDOT^0$ reduction/oxidation was involved to contribute for the capacitance. The obtained effective capacitance of K^+-SCISEs exponentially increases as the frequency decreases. As shown in Figure 6g,h, the logarithmic effective capacitance logC_{ec} of K^+-SCISEs with CWEs, 1, 5, and 10 mC PEDOT(PSS) solid contact covered with spin-coated membrane with respect to log$f$ gives a linear response in the range of 1 MHz to 10 Hz with a slope of *ca.* −0.97. At low frequencies ranging from 1 Hz to 10 mHz, the linear slope is suppressed, and this may due to the reversible solid contact $PEDOT^+/PEDOT^0$ oxidation/reduction process which is limited by the Warburg diffusion process of K^+ through PEDOT solid contact, as well as across the membrane and interfaces.[21,24,38]

The EIS excitation amplitude impact on the effective capacitance C_{ec} of PEDOT-based K^+-SCISEs with 5 mC PEDOT(PSS) covered with spin-coated membrane *vs* log$f$ is shown in Figure 7a. The logarithmic effective capacitance logC_{ec} *vs* log$f$ clearly shows that the effective capacitance of

https://doi.org/10.1021/acsmeasuresciau.4c00093
ACS Meas. Sci. Au 2025, 5, 216−225

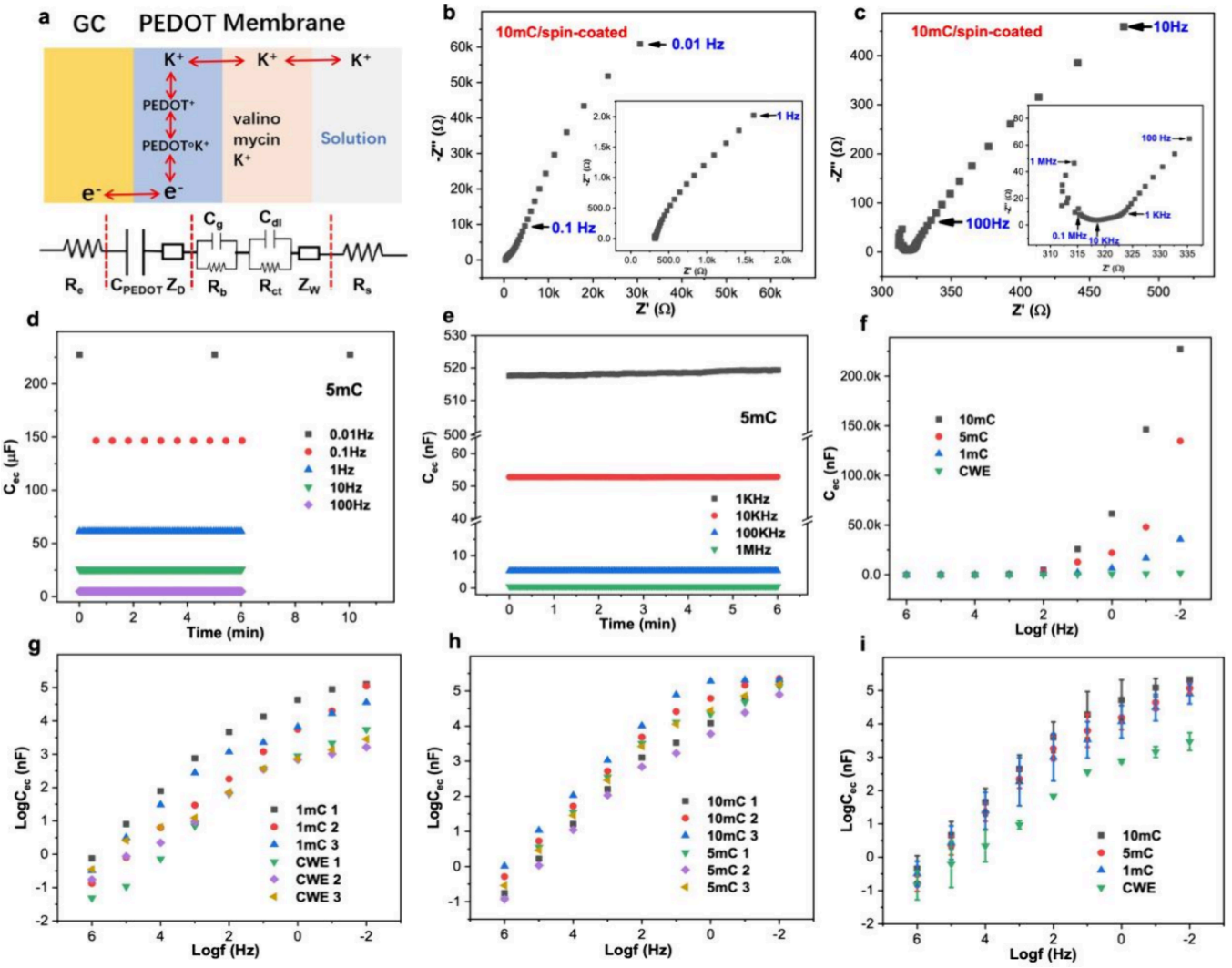

Figure 6. (a) Schematic picture of the K^+ ion-transfer mechanism of PEDOT-based SCISEs and the corresponding equivalent electrical circuit of PEDOT-based SCISEs[17]. (b, c) Electrochemical impedance spectrum of K^+-SCISEs with 10 mC PEDOT(PSS) and spin-coated membrane performed in 0.1 M KCl with frequency conversion from 1 MHz to 10 mHz. Figure 1b,c insets are the partial impedance enlargement. EIS effective capacitance C_{ec} of PEDOT-based K^+-SCISEs with 5 mC PEDOT(PSS) as solid contact, CWE covered with spin-coated membrane applied with frequency ranging from (d) 10 mHz to 100 Hz and (e) 1 kHz to 1 MHz *vs* time performed in 0.1 M KCl. (f) C_{ec} *vs* log*f*. LogC_{ec} of K^+-SCISEs with (g) CWE and 1 mC and (h) 5 and 10 mC PEDOT(PSS) covered with spin-coated membrane *vs* log*f*. The corresponding logC_{ec} of the K^+-SCISEs (Figure 7g,h) *vs* log*f* with error bar (n = 3) for each type of electrode (i). The applied EIS single frequency ranges from 1 MHz decreases by a factor of 10 to 10 mHz.

PEDOT-based K^+-SCISEs increases as the applied EIS single frequency decreases, ranging from 1 MHz to 10 mHz (Figure 7b,c). Inset is the partial enlargement of C_{ec} *vs* log*f* with error bar. At each excitation amplitude, it turns out to be stable and rather reproducible effective capacitance for 5 mC PEDOT-based K^+-SCISEs in 0.1 M KCl (Figure 7c). The linear slope of logC_{ec} *vs* log*f* for 5 mC PEDOT-based K^+-SCISEs in the range of 1 MHz to 10 Hz maintains *ca.* −0.94 when applied with multiple excitation amplitude parameters. At low frequencies ranging from 1 Hz to 10 mHz, the linear slope is suppressed to −0.23 (Figure 7d). Thus, the received EIS effective capacitance of 5 mC PEDOT-based K^+-SCISEs in 0.1 M KCl is dependent on the applied frequency and independent of the excitation amplitude (Figure 7c,d).

4. CONCLUSIONS

The performance of the single-frequency effective capacitance C_{ec} and membrane resistance Z for K^+-SCISEs with PEDOT as solid contact covered with drop-cast or spin-coated membrane was studied. In place of utilizing the impedance real part Z' of the traditional electrochemical impedance spectrum at semicircle high frequency, the membrane resistance corresponding to the impedance absolute value Z of K^+-SCISEs was recorded constantly as the KCl aqueous solution diluted with water was applied with high frequency. At high frequencies, the membrane resistance Z increases as the concentration of KCl aqueous solution decreases. Electrodes with drop-cast membrane (MΩ) give resistance of larger magnitude than the spin-coated electrode (hundreds Ω to 10 KΩ). For K^+-SCISEs covered with drop-cast (100 KΩ−MΩ) or spin-coated membrane (*ca.* 10 KΩ), the corresponding membrane resistance increases starting from $10^{-3.5}$ or 10^{-3} M KCl. As

https://doi.org/10.1021/acsmeasuresciau.4c00093
ACS Meas. Sci. Au 2025, 5, 216−225

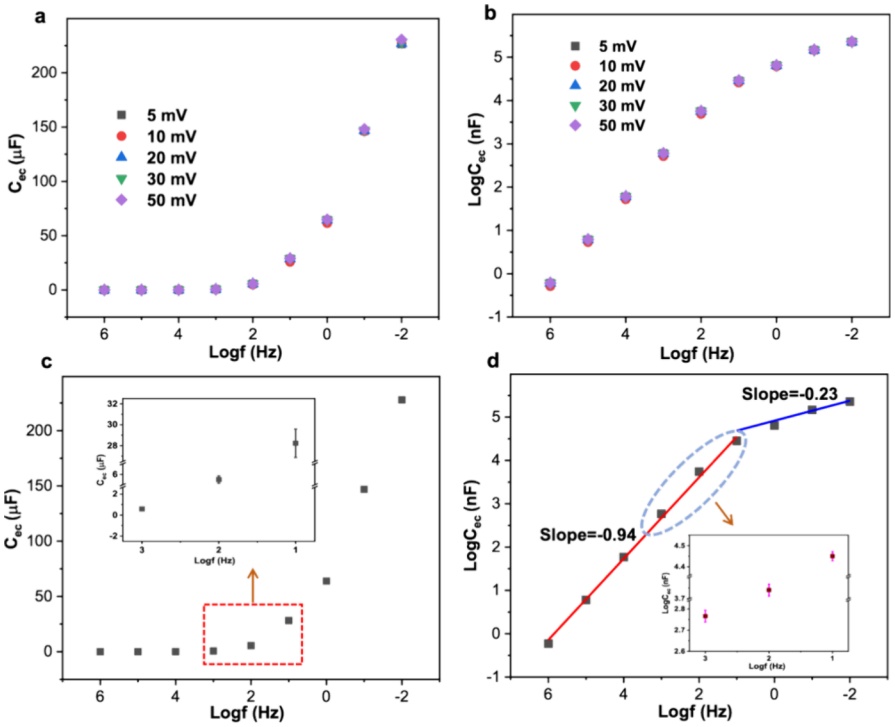

Figure 7. (a) EIS excitation amplitude impact on the effective capacitance C_{ec} of the PEDOT-based K^+-SCISE with 5 mC PEDOT(PSS) solid contact and spin-coated membrane applied with single frequency *vs* log*f* performed in 0.1 M KCl. (b) logC_{ec} *vs* log*f*. (c) C_{ec} of the K^+-SCISE (Figure 7a) with variable excitation amplitudes *vs* log*f* with error bar, inset is the enlarged section. (d) The corresponding logC_{ec} *vs* log*f* with error bar, inset is the partial enlargement.

the logarithmic activity of primary ion K^+ was diluted from −1 to −5, the membrane resistance *Z* of K^+-SCISEs is dependent on the concentration of KCl and also the thickness of the membrane. As the resistance of K^+-SCISEs with spin-coated membrane was reduced to hundreds Ω in 0.1 M KCl, the logarithmic effective resistance log*Z* of K^+-SCISEs is linearly proportional to loga_{K+} in the range of −1 to −3.4, providing a possibility of utilizing membrane resistance *Z* as an analytical signal for SCISEs in pure KCl aqueous solution. Furthermore, the membrane resistance *Z* is independent of applied high frequencies.

The effective capacitance C_{ec} of K^+-SCISEs with the spin-coated membrane was recorded with time in 0.1 M KCl applied with single frequency ranging from 1 MHz and it decreases by a factor of 10 to 10 mHz. A stable and reproducible effective capacitance was obtained in 6 min. The effective capacitance of K^+-SCISEs with a spin-coated membrane exponentially increases along with frequency. The logarithmic effective capacitance logC_{ec} gives a linear response with respect to log*f* in the range of 1 MHz to 10 Hz with a slope of *ca.* −0.97. At low frequencies ranging from 1 Hz to 10 mHz, the linear slope was suppressed, where Warburg diffusion takes effect. In comparison with the applied frequency, the effect of the EIS excitation amplitude on the effective capacitance of PEDOT-based K^+-SCISEs is almost negligible.

■ ASSOCIATED CONTENT

Supporting Information

The Supporting Information is available free of charge at https://pubs.acs.org/doi/10.1021/acsmeasuresciau.4c00093.

Potentiometric calibration curve of K^+-SCISEs covered with valinomycin membrane (PDF)

■ AUTHOR INFORMATION

Corresponding Author

Tingting Han − *Center for Advanced Analytical Science, Guangzhou Key Laboratory of Sensing Materials & Devices, Guangdong Engineering Technology Research Center for Photoelectric Sensing Materials & Devices, Key Laboratory of Optoelectronic Materials and Sensors in Guangdong Provincial Universities, School of Chemistry and Chemical Engineering, Guangzhou University, Guangzhou 510006, P.R. China;* orcid.org/0000-0002-6851-1080; Email: tinghan@gzhu.edu.cn

Authors

Sini Chen − *Center for Advanced Analytical Science, Guangzhou Key Laboratory of Sensing Materials & Devices, Guangdong Engineering Technology Research Center for Photoelectric Sensing Materials & Devices, Key Laboratory of Optoelectronic Materials and Sensors in Guangdong Provincial Universities, School of Chemistry and Chemical Engineering, Guangzhou University, Guangzhou 510006, P.R. China*

Tao Song − *State Key Laboratory of Pulp and Paper Engineering, South China University of Technology, Guangzhou 510640, P.R. China;* orcid.org/0000-0002-9389-7595

Dongxue Han − *Center for Advanced Analytical Science, Guangzhou Key Laboratory of Sensing Materials & Devices, Guangdong Engineering Technology Research Center for Photoelectric Sensing Materials & Devices, Key Laboratory of Optoelectronic Materials and Sensors in Guangdong Provincial Universities, School of Chemistry and Chemical*

https://doi.org/10.1021/acsmeasuresciau.4c00093
ACS Meas. Sci. Au 2025, 5, 216−225

Engineering, Guangzhou University, Guangzhou 510006, P.R. China; orcid.org/0000-0002-7343-2221

Li Niu − *Center for Advanced Analytical Science, Guangzhou Key Laboratory of Sensing Materials & Devices, Guangdong Engineering Technology Research Center for Photoelectric Sensing Materials & Devices, Key Laboratory of Optoelectronic Materials and Sensors in Guangdong Provincial Universities, School of Chemistry and Chemical Engineering, Guangzhou University, Guangzhou 510006, P.R. China; School of Chemical Engineering and Technology, Sun Yat-sen University, Zhuhai 519082, P.R. China;* orcid.org/0000-0003-3652-2903

Complete contact information is available at: https://pubs.acs.org/10.1021/acsmeasuresciau.4c00093

Author Contributions

CRediT: **Tingting Han** conceptualization, data curation, formal analysis, funding acquisition, investigation, methodology, project administration, resources, supervision, validation, writing - original draft, writing - review & editing; **Sini Chen** investigation, methodology; **Tao Song** data curation, investigation; **Dongxue Han** conceptualization, investigation, project administration, resources, supervision; **Li Niu** methodology, project administration, resources, software, supervision.

Notes

The authors declare no competing financial interest.

■ ACKNOWLEDGMENTS

The authors are grateful to Prof. Johan Bobacka (Åbo Akademi University, Turku, Finland) for his valuable discussions and constructive suggestions on EIS characterization of SCISEs. This work was supported by the National Natural Science Foundation of China (22204026), the Science and Technology Research Project of Guangzhou (202201000002 and 2023A03J0030), the Key Laboratory of Optoelectronic Materials and Sensors of Guangdong Province (2023KSYS008) and Department of Science & Technology of Guangdong Province (2022A156).

■ REFERENCES

(1) Mikhelson, K. N. *Ion-Selective Electrodes*; Springer, 2011.
(2) Bakker, E.; Bühlmann, P.; Pretsch, E. Carrier-based ion-selective electrodes and bulk optodes. 1. General characteristics. *Chem. Rev.* **1997**, *97*, 3083−3132.
(3) Bühlmann, P.; Pretsch, E.; Bakker, E. Carrier-based ion-selective electrodes and bulk optodes. 2. Ionophores for potentiometric and optical sensors. *Chem. Rev.* **1998**, *98*, 1593−1687.
(4) Bobacka, J.; Ivaska, A.; Lewenstam, A. Potentiometric ion sensors. *Chem. Rev.* **2008**, *108*, 329−351.
(5) Lindner, E.; Gyurcsanyi, R. E. Quality control criteria for solid-contact, solvent polymeric membrane ion-selective electrodes. *J. Solid. State Electrochem.* **2009**, *13*, 51−68.
(6) Michalska, A. All-solid-state ion-selective and all-solid-state reference electrodes. *Electroanal.* **2012**, *24*, 1253−1265.
(7) Cattrall, R. W.; Freiser, H. Coated Wire Ion-Selective Electrodes. *Anal. Chem.* **1971**, *43*, 1905−1906.
(8) Tang, Y.; Zhong, L.; Wang, W.; He, Y.; Han, T.; Xu, L.; Mo, X.; Liu, Z.; Ma, Y.; Bao, Y.; Gan, S.; Niu, L. Recent Advances in Wearable Potentiometric pH Sensors. *Membranes* **2022**, *12*, 504.
(9) Zhou, M.; Gan, S.; Cai, B.; Li, F.; Ma, W.; Han, D.; Niu, L. Effective solid contact for ion-selective electrodes: tetrakis(4-chlorophenyl)borate (TB^-) anions doped nanocluster films. *Anal. Chem.* **2012**, *84*, 3480−3483.
(10) Cadogan, A.; Gao, Z.; Lewenstam, A.; Ivaska, A.; Diamond, D. All-Solid-State Sodium-Selective Electrode Based on a Calixarene Ionophore in a Poly(Vinyl Chloride) Membrane with a Polypyrrole Solid Contact. *Anal. Chem.* **1992**, *64*, 2496−2501.
(11) Lyu, Y.; Han, T.; Zhong, L.; Tang, Y.; Xu, L.; Ma, Y.; Bao, Y.; Gan, S.; Bobacka, J.; Niu, L. Coulometric ion sensing with Li^+-selective $LiMn_2O_4$ electrodes. *Electrochem. Commun.* **2022**, *139*, No. 107302.
(12) Crespo, G.; Macho, S.; Bobacka, J.; Rius, F. X. Transduction Mechanism of Carbon Nanotubes in Solid-Contact Ion-Selective Electrodes. *Anal. Chem.* **2009**, *81*, 676−681.
(13) Kozna, J.; Tapp, S.; Gyurcsányi, R. E. TEMPO-Functionalized Carbon Nanotubes for Solid-Contact Ion-Selective Electrodes with Largely Improved Potential Reproducibility and Stability. *Anal. Chem.* **2022**, *94*, 8249−8257.
(14) Papp, S.; Bojtar, M.; Gyurcsányi, R. E.; Lindfors, T. Potential Reproducibility of Potassium-Selective Electrodes Having Perfluorinated Alkanoate Side Chain Functionalized Poly(3,4-ethylenedioxythiophene) as a Hydrophobic Solid Contact. *Anal. Chem.* **2019**, *91*, 9111−9118.
(15) Iglehart, M. L.; Buck, R. P.; Horvai, G.; Pungor, E. Plasticized poly(vinyl chloride) properties and characteristics of valinomycin electrodes. Current-time responses to voltage steps. *Anal. Chem.* **1988**, *60*, 1018−1022.
(16) Bobacka, J. Potential Stability of All-Solid-State Ion-Selective Electrodes Using Conducting Polymers as Ion-to-Electron Transducers. *Anal. Chem.* **1999**, *71*, 4932−4937.
(17) Bobacka, J.; Lewenstam, A.; Ivaska, A. Equilibrium potential of potentiometric ion sensors under steady-state current by using current-reversal chronopotentiometry. *J. Electroanal. Chem.* **2001**, *509*, 27−30.
(18) Zdrachek, E.; Bakker, E. Potentiometric sensing. *Anal. Chem.* **2021**, *93*, 72−102.
(19) Yin, T.; Han, T.; Li, C.; Qin, W.; Bobacka, J. Real-time monitoring of the dissolution of silver nanoparticles by using a solid-contact Ag^+-selective electrode. *Anal. Chim. Acta* **2020**, *1101*, 50−57.
(20) Rousseau, C. R.; Chipangura, Y. E.; Stein, A.; Bühlmann, P. Effect of Ion Identity on Capacitance and Ion-to-Electron Transduction in Ion-Selective Electrodes with Nanographite and Carbon Nanotube Solid Contacts. *Langmuir* **2024**, *40*, 1785−1792.
(21) Toth, K.; Graf, E.; Horvai, G.; Pungor, E.; Buck, R. P. Plasticized Poly(vinyl chloride) Properties and Characteristics of Valinomycin Electrodes. 2. Low-Frequency, Surface-Rate, and Warburg Impedance Characteristics. *Anal. Chem.* **1986**, *58*, 2741−2744.
(22) Bobacka, J.; Lewenstam, A.; Ivaska, A. Electrochemical impedance spectroscopy of oxidized poly(3,4-ethylenedioxythiophene) film electrodes in aqueous solutions. *J. Electroanal. Chem.* **2000**, *489*, 17−27.
(23) Mattinen, U.; Rabiej, S.; Lewenstam, A.; Bobacka, J. Impedance study of the ion-to-electron transduction process for carbon cloth as solid-contact material in potentiometric ion sensors. *Electrochim. Acta* **2011**, *56*, 10683−10687.
(24) Nahir, T. M.; Buck, R. P. Steady-state-current impedance spectroscopy of plasticized PVC membranes containing neutral ion carriers. *Electrochim. Acta* **1993**, *38*, 2691−2697.
(25) Bobacka, J. Perspective on the coulometric transduction principle for ion-selective electrodes. *Sens. Actuators B: Chem.* **2024**, *410*, No. 135674.
(26) Hupa, E.; Vanamo, U.; Bobacka, J. Novel ion-to-electron transduction principle for solid-contact ISEs. *Electroanal.* **2015**, *27*, 591−594.
(27) Vanamo, U.; Hupa, E.; Yrjana, V.; Bobacka, J. New signal readout principle for solid-contact ion-selective electrodes. *Anal. Chem.* **2016**, *88*, 4369−4374.
(28) Bonda, A. V.; Keresten, V. M.; Mikhelson, K. N. Registration of small (below 1%) changes of calcium ion concentration in aqueous solutions and in serum by the constant potential coulometric method. *Sens. Actuators B: Chem.* **2022**, *354*, No. 131231.

(29) Cuartero, M.; Bishop, J.; Walker, R.; Acres, R. G.; Bakker, E.; Marc, R. D.; Crespo, G. A. Evidence of double layer/capacitive charging in carbon nanomaterial-based solid contact polymeric ion-selective electrodes. *Chem. Commun.* **2016**, *52*, 9703−9706.
(30) Guo, J.; Amemiya, S. Voltammetric Heparin-Selective Electrode Based on Thin Liquid Membrane with Conducting Polymer-Modified Solid Support. *Anal. Chem.* **2006**, *78*, 6893−6902.
(31) Han, T.; Mattinen, U.; Bobacka, J. Improving the sensitivity of solid-contact ion-selective electrodes by using coulometric signal transduction. *ACS Sens.* **2019**, *4*, 900−906.
(32) Nussbaum, R.; Jeanneret, S.; Bakker, E. Ultrasensitive sensing of pH and fluoride with enhanced constant potential coulometry at membrane electrodes. *Anal. Chem.* **2024**, *96*, 6436−6443.
(33) Horvai, G.; Graf, E.; Toth, K.; Pungor, E.; Buck, R. P. Plasticized Poly(vinyl chloride) Properties and Characteristics of Valinomycin Electrodes. 1. High-Frequency Resistances and Dielectric Properties. *Anal. Chem.* **1986**, *58*, 2735−2740.
(34) Kovács, M. M.; Höfler, L. Effect of Kinetic and Thermodynamic Properties of Solid Contact Ion-Selective Electrodes on the Electrochemical Impedance Spectroscopy Response. *J. Electrochem. Soc.* **2022**, *169*, No. 026509.
(35) Marco, R. D.; Pejcic, B. Electrochemical Impedance Spectroscopy and X-ray Photoelectron Spectroscopy Study of the Response Mechanism of the Chalcogenide Glass Membrane Iron(III) Ion-Selective Electrode in Saline Media. *Anal. Chem.* **2000**, *72*, 669−679.
(36) Radu, A.; Ivanova, S. A.; Bator, B. P.; Danielewski, M.; Bobacka, J.; Lewenstam, A.; Diamond, D. Diagnostic of functionality of polymer membrane-based ion selective electrodes by impedance spectroscopy. *Anal. Methods* **2010**, *2*, 1490−1498.
(37) Grzeszcuzuk, M.; Bobacka, J.; Ivaksa, A. Ion transfer at a poly(3-octylthiophene) film electrode. *J. Electroanal. Chem.* **1993**, *362*, 287−289.
(38) Bobacka, J.; Grzeszczuk, M.; Ivaksa, A. Electrochemical study of poly(3-octylthiophene) film electrodes. Impedance of the polymer film semiconductor electrolyte interface. *Electrochim. Acta* **1992**, *37*, 1759−1765.
(39) Gao, Z.; Bobacka, J.; Ivaksa, A. Electrochemical impedance spectroscopy of cobalt(II)-hexacyanoferrate film modified electrodes. *Electrochim. Acta* **1993**, *38*, 379−385.
(40) Shvarev, A. E.; Rantsan, D. A.; Mikhelson, K. N. Potassium-selective conductometric sensor. *Sens. Actuators B: Chem.* **2001**, *76*, 500−505.
(41) Ivanova, A.; Mikhelson, K. Electrochemical Properties of Nitrate-Selective Electrodes: The Dependence of Resistance on the Solution Concentration. *Sensors* **2018**, *18*, 2062.
(42) Kondratyeva, Y. O.; Solovyeva, E. V.; Khripoun, G. A.; Mikhelson, K. N. Non-constancy of the bulk resistance of ionophore-based ion-selective electrode: A result of electrolyte co-extraction or of something else? *Electrochim. Acta* **2018**, *259*, 458−465.
(43) Kalinichev, A. V.; Solovyeva, E. V.; Ivanova, A. R.; Khripoun, G. A.; Mikhelson, K. N. Non-constancy of the bulk resistance of ionophore-based Cd^{2+}-selective electrode: A correlation with the water uptake by the electrode membrane. *Electrochim. Acta* **2020**, *334*, No. 135541.
(44) Keresten, V.; Lazarev, F.; Mikhelson, K. N. Transfer of Sodium Ion across Interface between Na^{+}-Selective Electrode Membrane and Aqueous Electrolyte Solution: Can We Use Nernst Equation If Current Flows through Electrode? *Membranes* **2024**, *14*, 74.
(45) Keresten, V.; Solovyeva, E.; Mikhelson, K. N. The Origin of the Non-Constancy of the Bulk Resistance of Ion-Selective Electrode Membranes within the Nernstian Response Range. *Membranes* **2021**, *11*, 344.
(46) Han, T.; Song, T.; Bao, Y.; Wang, W.; He, Y.; Liu, Z.; Gan, S.; Han, D.; Bobacka, J.; Niu, L. Fast and sensitive coulometric signal transduction for ion-selective electrodes by utilizing a two-compartment cell. *Talanta* **2023**, *262*, No. 124623.
(47) Han, T.; Chen, S.; Yang, S.; Song, T.; Lin, X.; Qin, Y.; Han, D.; Bobacka, J.; Niu, L. Determination of silver ions in distilled water by stripping voltammetry at a Nafion-coated gold electrode in combination with quartz crystal microbalance and electrochemical impedance spectroscopy. *Talanta* **2025**, *282*, No. 127006.
(48) Bobacka, J.; Ivaska, A.; Lewenstam, A. Plasticizer-free all-solid-state potassium-selective electrode based on poly(3-octylthiophene) and valinomycin. *Anal. Chim. Acta* **1999**, *385*, 195−202.
(49) Lazanas, A. C.; Prodromidis, M. I. Electrochemical Impedance Spectroscopy-A Tutorial. *ACS meas. Sci. Au* **2023**, *3*, 162−193.

https://doi.org/10.1021/acsmeasuresciau.4c00093
ACS Meas. Sci. Au 2025, 5, 216−225